

Cobalt catalysts prepared from hydrotalcite precursors and tested in methane steam reforming

Alessandra Fonseca Lucrédio, Elisabete Moreira Assaf*

Instituto de Química de São Carlos, Universidade de São Paulo, Av. Trabalhador São-carlense, 400, 13566-590 São Carlos, SP, Brazil

Received 22 September 2005; accepted 24 October 2005

Available online 6 January 2006

Abstract

Catalysts were prepared from hydrotalcite precursors, then characterized and tested for methane steam reforming. The precursors were synthesized by the traditional technique, based on co-precipitation of Co, Mg and Al nitrates with carbonate; by co-precipitation of Mg and Al nitrates with pre-synthesized cobalt chelate and by anion-exchange of hydrotalcite NO_3^- with cobalt chelate. The oxides were analyzed by atomic absorption spectrophotometry, thermogravimetric analysis, X-ray diffraction, temperature programmed reduction with H_2 , catalytic tests and elemental analysis. The catalysts, tested in methane steam reforming, showed stability and activity at a feed molar ratio $\text{H}_2\text{O}:\text{CH}_4 = 2:1$.

© 2005 Elsevier B.V. All rights reserved.

Keywords: Anionic clays; Layered double hydroxides; Cobalt catalysts; Hydrogen production

1. Introduction

Reforming of hydrocarbons, particularly methane steam reforming, is a useful process for hydrogen production. Steam reforming reactions are outlined in reactions (1) and (2) [1]:



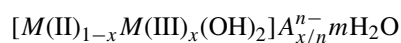
Supported nickel catalysts are used in industry, although these catalysts require a high steam:methane molar ratio (3.0–3.5) in the feed, in order to favor the gasification of carbon species and avoid carbon formation reaction (3), which would lead to catalyst deactivation [1,2]. Other metals such as Rh, Ru, Pd, Pt and Co are also active for methane steam reforming [3].



It is known that metallic species highly dispersed over supports avoid becoming sintered during the process [4], so that the rate of carbon deposition is reduced, since large metal particles stimulate carbon formation [5]. Supported metal catalysts are normally prepared by impregnation of various supports.

However, this method may produce some heterogeneity in the distribution of metal on the surface, and the uneven dispersion of metallic species could favor carbon formation [4]. The use of precursors in which the metal is homogeneously distributed throughout the catalytic structure, may result, after calcination and reduction, in the formation of highly-dispersed and stable metal particles on the surface. Hydrotalcites have been found, after thermal treatment, to afford a homogeneous dispersion of the metal and a better resistance to sintering than the corresponding supported catalysts [6], and some authors have reported that the use of hydrotalcite precursors minimizes carbon formation, since all the cations are homogeneously distributed across the brucite-type sheets within the hydrotalcite anionic clay structure [4].

Hydrotalcites, a family of anionic clays, are known as layered double hydroxides (LDHs). They may be represented by the general formula:



and consist of layers of brucite, $M(\text{II})(\text{OH})_2$, which, as a result of partial substitution of divalent by trivalent cations, acquire excess positive charge. This excess charge is compensated by the incorporation of anions into the interlayer space. An important feature of these compounds is the relative facility of anion exchange [7]. There is practically no restriction on the nature of

* Corresponding author. Tel.: +55 16 33739918; fax: +55 16 33739952.
E-mail address: eassaf@iqsc.usp.br (E.M. Assaf).

the anions, except that they should not form strong complexes with the cations present. It is known that the interlayer space can be used to introduce metals in the anionic form (chromates, chelates and others) [8]. Tsyganok et al. [9,10] reported a novel method of hydrotalcite synthesis, in which they suggested the introduction of nickel into the MgAl (LDH), using the fact that Ni(II) reacts with the anionic chelating agent EDTA⁻⁴, making the highly stable complex [Ni(EDTA)]⁻².

In a previous paper [11], we reported the application of nickel hydrotalcites, prepared by various methods [10], to steam reforming of methane at different molar steam:methane ratios in the feed (4, 2 and 0.5:1), obtaining high activity without deactivation during the time of reaction.

Makoa et al. [3], evaluated Co/Mg/Al₂O₃ catalysts in the partial oxidation of methane under high pressure, and found that the catalyst was deactivated after a period of time, due to coke formation.

Ruckenstein and Wang [12] studied cobalt catalysts on different supports (MgO, CaO and SiO₂) in CO₂ reforming of methane, where the reduced catalyst Co/MgO showed a high activity and stability, without deactivation, for 110 h of reaction. Nevertheless, the high calcining temperatures led to solid solution formation, with strong metal-support interactions that hindered subsequent reduction.

In light of the above points, the goal of this work was the preparation and characterization of catalysts from cobalt hydrotalcite precursors obtained by the traditional technique and by chelation. These catalysts were tested on the reaction of methane steam reforming, with two molar ratios of steam:methane in the feed.

2. Experimental

2.1. Synthesis

The hydrotalcite precursor containing cobalt was prepared by three different methods: traditional, co-precipitation and anion-exchange, based on the work of Tsyganok et al. [10]. Precipitation was performed at 63 °C and pH 10, the latter being controlled adding 1 M aqueous NaOH solution.

2.1.1. Traditional technique (Tr-CoMgAl-CO₃)

A Co-containing MgAl layered double hydroxide was prepared by dropwise addition of an aqueous solution (100 mL) containing Co(II), Mg(II) and Al(III) nitrates (5, 25 and 10 mmol) to a continually stirred solution of sodium carbonate (30 mmol in 200 mL). The resulting suspension was stirred at 63 °C for 1 h. Next, the precipitate was aged at the same temperature for 18 h without stirring. The pale rose-colored precipitate was separated by filtration, rinsed with deionized water (until complete removal of Na⁺ ions), dried in air at 80 °C for 24 h and reserved.

2.1.2. Chelation-based techniques

A cobalt complex chelate was utilized for the syntheses below. It was prepared by adding cobalt nitrate solution (50 mmol in 100 mL of water) to tetrasodium EDTA solution

(50 mmol in 100 mL of water) at 63 °C. This chelated solution was denominated (CoY)⁻² [10].

- Co-precipitation method (Cp-MgAl-CoY): An aqueous solution (100 mL) of Mg(II) and Al(III) nitrates (30 and 10 mmol) was added dropwise to stirred (CoY)⁻² solution, at pH 10. The resulting suspension was stirred at 63 °C for 1 h, and then the precipitate was aged at the same temperature for 18 h without stirring and received the same treatment as in the traditional technique.
- Anion-exchange method (Ae-MgAl-CoY): In this method, the hydrotalcite MgAl-LDH was first obtained by the addition of Mg(II) and Al(III) nitrates (30 and 10 mmol dissolved in 100 mL of water) to 1 M aqueous NaOH solution, with stirring. The suspension was stirred for 1 h, and then aged as in the others techniques. (CoY)⁻² solution was added to this suspension, which was stirred at room temperature. The suspension was then stirred for 24 h at room temperature and the precipitate received the same treatment as above.

The hydrotalcites were calcined at 500 °C in air for 15 h, and denominated Tr-LDH calcined, Cp-LDH calcined and Ae-LDH calcined, according to the hydrotalcite precursor [10].

2.2. Characterization techniques

The chemical composition of Co-LDH was determined in a Hitachi Z-8100 atomic-absorption spectrophotometer with lamp current 12.5 mA, wavelength 240.7 nm and a flame of Ar/C₂H₂ (2.2 L min⁻¹).

The thermogravimetric analysis of the samples was carried out in an ATG-Therma Analyst 2100 (TA Instruments) operated under a flow of N₂ in a temperature range of 25–1000 °C, at a heating rate of 10 °C min⁻¹.

X-ray diffraction patterns were collected at room temperature in a URD-6 Carl Zeiss diffractometer with Cu K α radiation ($\lambda = 1.54056 \text{ \AA}$). The spectra were scanned in the range $2\theta = 3\text{--}80^\circ$ at a rate of 2° min^{-1} .

Temperature-programmed reduction with hydrogen (H₂-TPR) of the catalysts was performed in a Micromeritics Chemisorb 2705, using 50 mg of catalyst and a temperature ramp from 25 to 1000 °C at 10 °C min⁻¹. A flow rate of the 30 mL min⁻¹ of 5% H₂/N₂ was used.

Carbon formation on the catalyst during tests of activity was measured by elemental analysis in an Elemental Analyzer CE1110, model CHNS-0, using 3 mg of the sample in a tin capsule, with the furnace at 1200 °C.

2.3. Catalytic tests

Catalytic activity was tested in a fixed-bed tubular quartz micro-reactor, so as to analyze the activity for hydrogen production, products distribution and carbon formation as a function of reaction time. Catalytic performance was tested with an apparatus consisting of flow controllers, the reactor unit, and the analytical system. The flow system consisted of a set of mass-flow controllers (Allborg, four channels), which accurately control

the flow of each feed gas (H_2 , N_2 , CH_4 , etc.) entering the reactor. The catalyst was placed in a quartz wool bed system inside a continuous flow micro-reactor (13 mm diameter). The operating temperature was controlled by a thermocouple placed inside the oven and close to the reactor wall, to assure precise temperature measurements during the pre-treatment and reaction steps. Prior to the reaction, 100 mg of the catalyst was introduced into the reactor and reduced in situ in flowing H_2 (50 mL min^{-1}) at 550°C ($10^\circ\text{C min}^{-1}$) for 1 h, to activate the catalyst. Next, the sample was heated to 750°C under a flow of pure N_2 . The reaction was started in a hydrogen free feed. The water was pumped to a vaporizer, where it was heated to 180°C and then fed to the reactor. The CH_4 flow was 40 mL min^{-1} and the feed molar ratios used were $H_2O_v:CH_4 = 2:1$, $W/F = 0.35 \text{ g h mol}^{-1}$ ($WHSV = 49 \text{ h}^{-1}$), which is stoichiometric for the reaction, and $H_2O_v:CH_4 = 0.5:1$, $W/F = 0.69 \text{ g h mol}^{-1}$ ($WHSV = 24 \text{ h}^{-1}$), an extreme feed ratio, where the methane is in large excess, to test the activity of the catalyst.

The analyses of the reactants and all the reaction products were carried out in-line by gas chromatography (Varian, Model 3800) with two thermal conductivity detectors. The reaction product stream was divided into two outlet streams by an automatic injection valve, which were analyzed differently in order to obtain accurate and complete quantification of the reaction products. One of these aliquots was used to analyze hydrogen and methane, which were separated in a $13\times$ molecular sieve packed column, using N_2 as carrier gas. The other aliquot was used to analyze CO_2 , CH_4 , CO and N_2 . Helium was used as the carrier gas and separation was performed in a $13\times$ molecular sieve and Porapak N packed columns. At the end of the catalytic test, the flow of H_2O/CH_4 was stopped and the catalyst was cooled under a N_2 stream and stored for further characterization by elemental analysis.

3. Results and discussion

3.1. Elemental composition

The composition of each hydrotalcite is shown in Table 1.

The quantity of water of hydration was calculated from the mass loss in thermogravimetric analysis.

Analysis of the elemental composition of all samples revealed that the atomic ratio Mg:Al (8:1) was higher than the starting value (Mg:Al = 3:1). This loss of aluminum ions was attributed by Tsyganok et al. [10] to the formation of water-soluble aluminates reaction (4) from aluminum hydroxide at the moderately high pH.

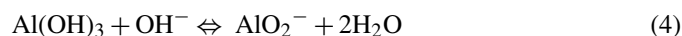


Table 1
Composition of hydrotalcites

Sample	Composition
Tr-LDH	$[Co_{0.07}Mg_{0.83}Al_{0.1}(OH)_2](CO_3)^{-2}_{0.05} \cdot 0.9H_2O$
Cp-LDH	$[Mg_{0.89}Al_{0.11}(OH)_2](CoY)^{-2}_{0.055} \cdot 0.65H_2O$
Ae-LDH	$[Mg_{0.89}Al_{0.11}9(OH)_2](CoY)^{-2}_{0.055} \cdot 0.25H_2O$

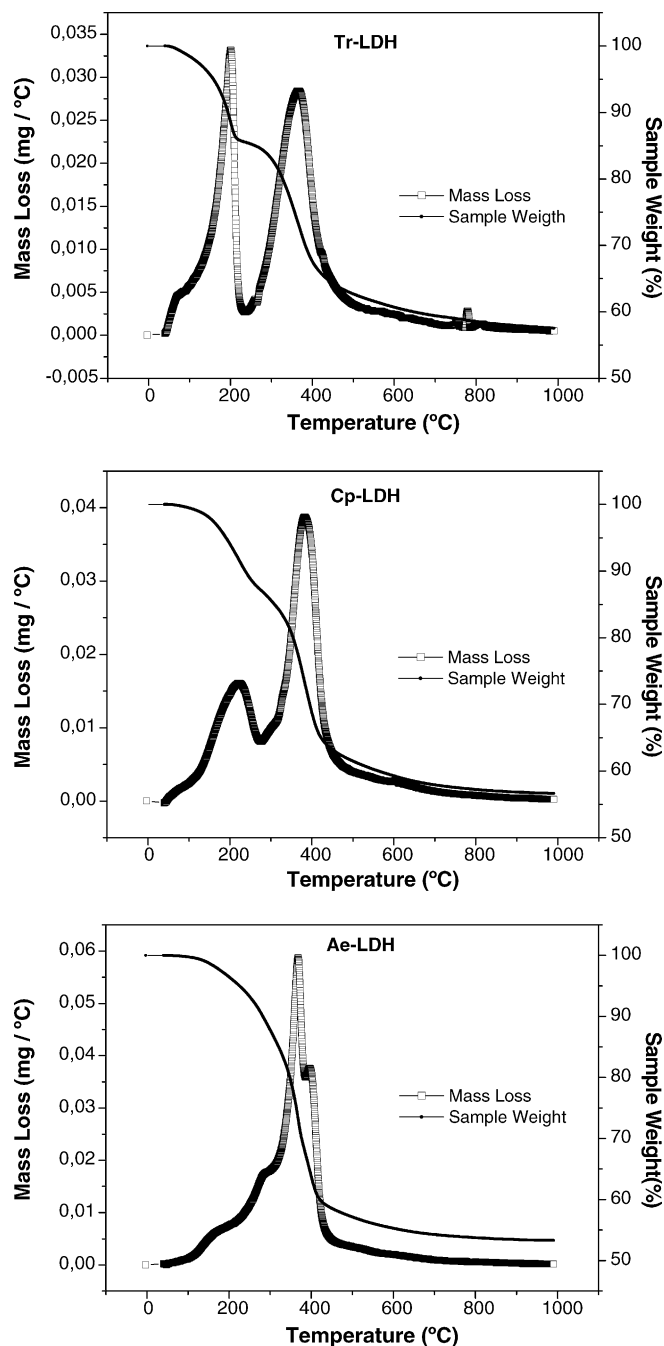


Fig. 1. TGA of Tr-LDH, Cp-LDH and Ae-LDH.

3.2. TGA measurements

In Fig. 1, the thermal decomposition of hydrotalcites is shown.

From the results of TGA, a marked difference in properties can be seen between cobalt-containing LDHs synthesized by intercalation and by traditional techniques.

Traditional MgAl-LDH exhibits thermal decomposition in two steps, as can be seen in Fig. 1. However, the difference in sample mass loss in step 1 ($40\text{--}240^\circ\text{C}$) and step 2 ($250\text{--}900^\circ\text{C}$) was not pronounced. Regarding the loss of mass, three peaks can be observed. A temperature around 80°C was sufficient for

removal of physisorbed water. The desorption of structural water required a higher temperature, about 200 °C. The third peak at 380 °C consists of simultaneous loss of water molecules, by decomposition of hydroxyl groups, and desorption of CO₂ [13].

Considering samples based on (CoY)²⁻, the sample Cp-LDH also revealed a two-step reduction in mass, while for sample Ae-LDH, only a single step reduction in mass can be seen. The loss of mass demonstrated three peaks for both Cp-LDH and Tr-LDH samples, the first two referring to physisorbed water (100 °C) and desorption of structural water (200 °C). The third peak, positioned around 400 °C, consists of simultaneous loss of water molecules from decomposition of hydroxyl groups, collapse of the layered structure and decomposition of entrapped (CoY)²⁻. In sample Ae-LDH, these steps can be seen separately. Also, it should be noted for that the two samples, Cp-LDH and Ae-LDH, the third peak is bigger than the first two, this being an indication of chelate incorporation [10].

3.3. X-ray diffraction (XRD)

Fig. 2 presents the XRD patterns of synthesized precursors and calcined samples. The hydrotalcite patterns show that all precursors produced peaks that are characteristic of hydrotalcite structure, and the traditional method led to the highest crystallinity. The thermal treatment resulted in changes of their phase structures, giving rise to segregated phases. Calcinations at 500 °C for 15 h resulted in the disappearance of part of the layered structure of hydrotalcite and the formation of peaks attributed to the Co₃O₄ and/or Co^{3+/2+} incorporated into the aluminum and magnesium oxide structure [14].

3.4. Temperature-programmed reduction (TPR)

The TPR patterns of calcined samples are presented in Fig. 3, where five reduction peaks can be seen.

The first peak at 145 °C, which is present only in Ae catalyst, can be attributed to the decomposition of Co(NO₃)₂ remaining on the hydrotalcite surface.

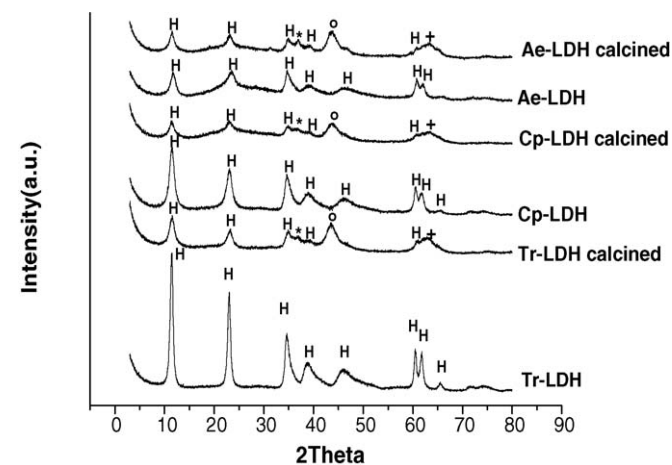


Fig. 2. X-ray diffraction patterns of hydrotalcite precursors and calcined samples (H, hydrotalcite; *, Co₃O₄ and/or MgCo₂O₄ and/or CoAl₂O₄; °, Co₃O₄ and/or MgCo₂O₄; +, (Co,Mg)O and/or MgO).

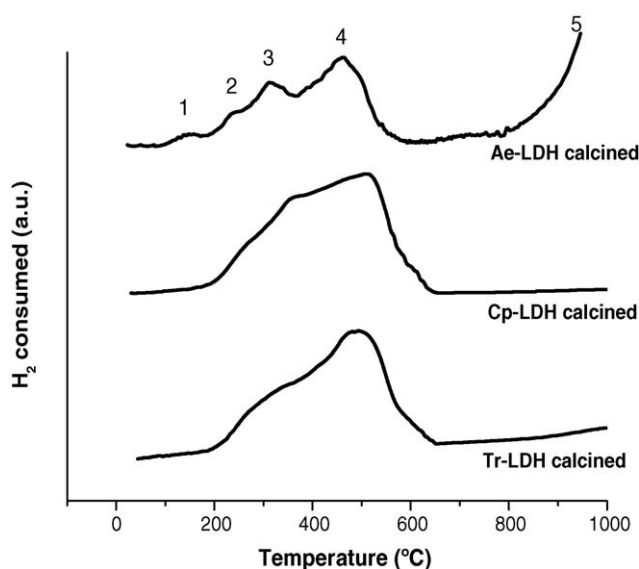


Fig. 3. Patterns of TPR of the calcined samples.

The second and third peaks, at 240 and 315 °C, are related to Co₃O₄ reduction. According to Khassin et al. [15], this can be reduced in two stages, at 250 and 350 °C, forming CoO and Co⁰, respectively.

The fourth peak, at 460 °C, can be attributed to the reduction of Co^{3+/2+} cations dissolved in the MgO and/or Al₂O₃ phase, according to XRD patterns and the results of Chmielarz et al. [13].

Peak 5, which is present only in the Ae catalyst, starting around 820 °C, is related to reduction of the solid solution (Co, Mg)O, formed by diffusion of CoO species into the MgO matrix. This assignment is according to Wang and Ruckenstein [16].

3.5. Catalytic tests

Fig. 4 presents the methane conversions with a feed of molar ratio H₂O_v:CH₄ = 2:1, W/F: 0.35 g h mol⁻¹ (WHSV = 49 h⁻¹) at

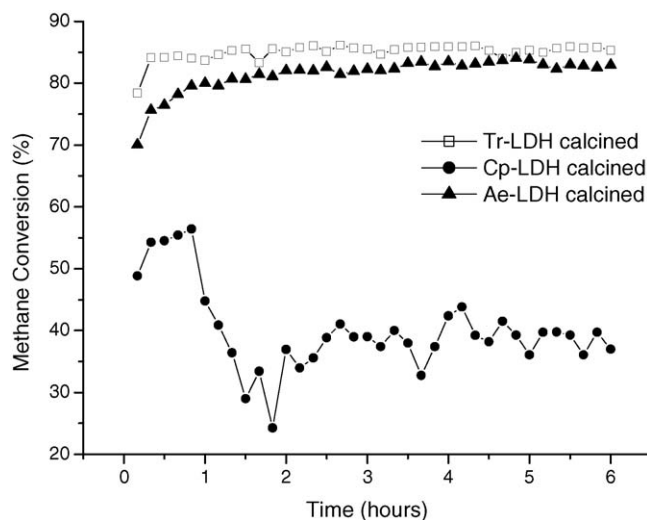


Fig. 4. Methane conversion for molar ratio of feed H₂O_v:CH₄ = 2:1.

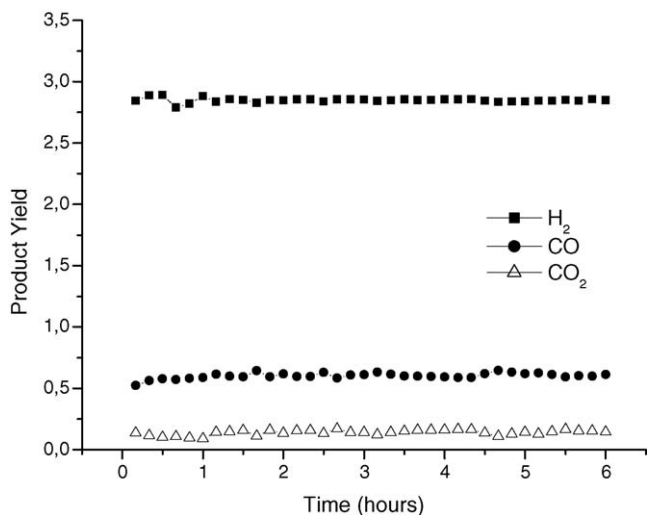


Fig. 5. Product yields for calcined Tr-LDH catalyst for molar ratio of feed $H_2O_v:CH_4 = 2:1$.

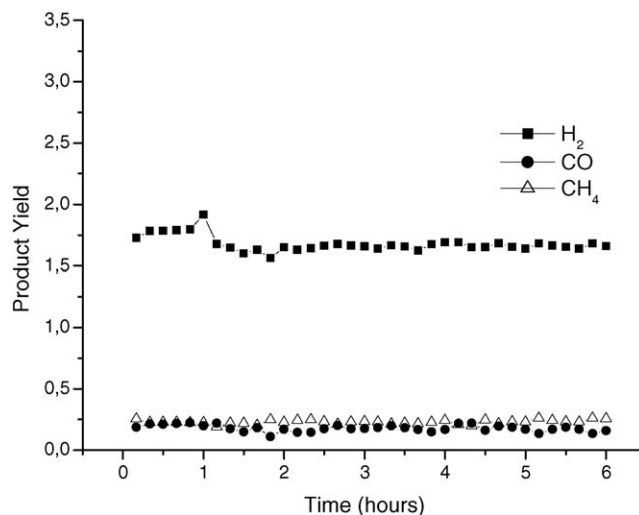


Fig. 6. Product yields for calcined Cp-LDH catalyst for molar ratio of feed $H_2O_v:CH_4 = 2:1$.

750 °C. Tr and Ae-catalysts showed good activity, with conversions around 80%, without deactivation, during 6 h of reaction. Cp-catalyst suffered an initial fall in conversion, which thereafter remained around 40%.

Figs. 5–7 show the product yields for the molar ratio H_2O/CH_4 of 2:1, calculated according to Eq. (1) and reactions (1) and (2).

$$Yield_i = \frac{\text{moles of product } i}{\text{moles of } CH_4 \text{ supplied}} \quad (1)$$

Table 2 presents the average H_2/CO molar composition and the amount of carbon formed on catalysts after 6 h of reaction with a feed molar ratio $H_2O_v:CH_4 = 2:1$. It can be seen that the catalysts produced high H_2/CO molar ratios, with a favoring of the shift reaction on calcined Cp-LDH catalyst reaction (2) and Fig. 6. Comparing the catalysts calcined Tr-LDH and calcined Ae-LDH, which achieved similar conversions, it was noted that the calcined Ae-LDH catalyst allowed a smaller amount of carbon to form (Fig. 7). However, the calcined Tr-LDH catalyst showed more selectivity to H_2 production (Fig. 5). The calcined Cp-LDH catalyst exhibited a fall in conversion in the two first hours of the reaction, which could be related to the oxidation of part of the cobalt active sites.

Fig. 8 presents the methane conversion with a feed molar ratio H_2O_v/CH_4 of 0.5:1. These tests were made so as to analyze the stability of the catalysts in extreme conditions. A slow deactivation tendency (carbon formation) was observed during the 6 h of tests, because the excess methane in the feed suffered decom-

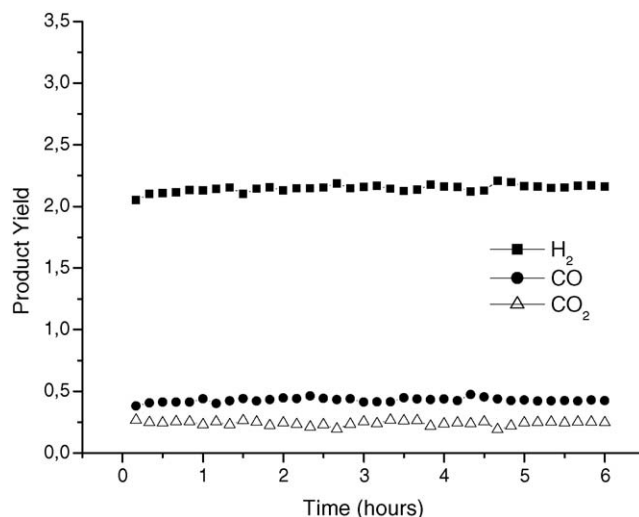


Fig. 7. Product yields for calcined Ae-LDH catalyst for molar ratio of feed $H_2O_v:CH_4 = 2:1$.

Table 2
Average H_2/CO molar composition of products and amount of carbon on catalyst (wt%) after 6 h of reaction with molar ratio $H_2O_v:CH_4 = 2:1$

Catalyst	H_2/CO (average)	Amount of carbon (%)
Tr-LDH calcined	4.8	6.4
Cp-LDH calcined	9.5	4.4
Ae-LDH calcined	5.1	2.2
Ae-LDH calcined (30h)	4.9	2.7

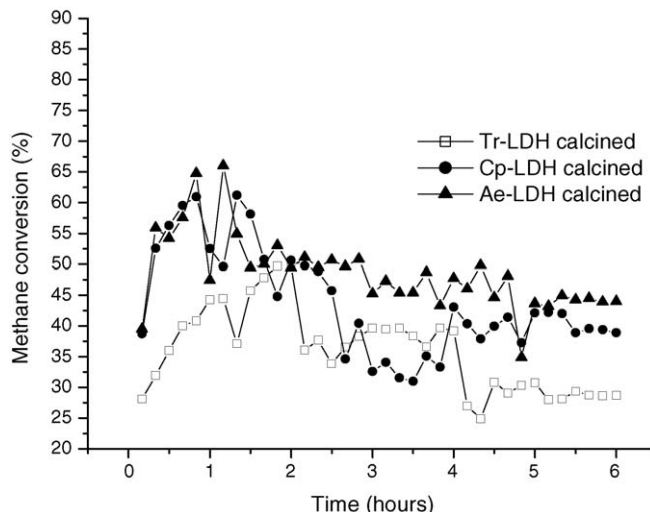


Fig. 8. Methane conversion for molar ratio of feed $H_2O_v:CH_4 = 0.5:1$.

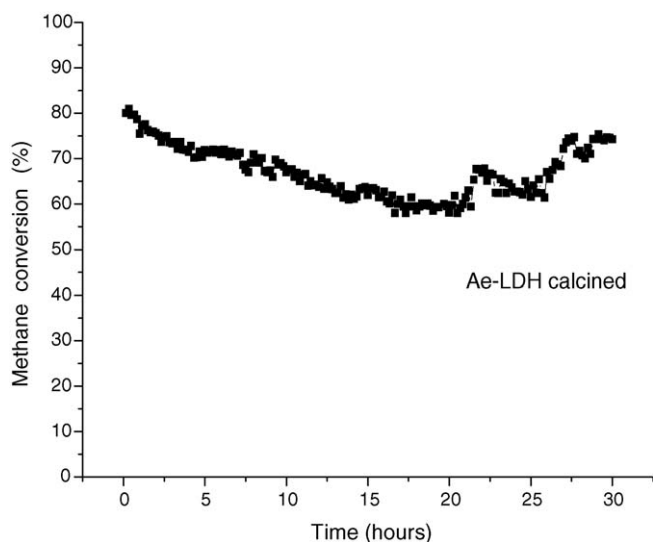


Fig. 9. Methane conversion for molar ratio of feed $\text{H}_2\text{O}_v:\text{CH}_4 = 2:1$ during 30 h of reaction.

position through dissociation reactions. Nevertheless, this result can be considered promising, taking into account the reactions conditions used.

As can be seen in Fig. 8, the calcined Cp-LDH now catalyses the conversion as well as the Tr and Ae catalysts, corroborating the hypothesis of oxidation of a part of the cobalt active sites in the reaction with molar ratio in the feed of $\text{H}_2\text{O}_v:\text{CH}_4 = 2:1$, presented in Fig. 4.

Still with respect to the stability of the catalysts, one test was carried out with calcined Ae-LDH catalyst, for a molar ratio in the feed of $\text{H}_2\text{O}_v:\text{CH}_4 = 2:1$, lasting 30 h. As can be seen in Fig. 9, the catalyst suffered deactivation during the first 20 h of the reaction (about 20%). Nevertheless, in the final 10 h it recovered the lost activity. After the test, this sample showed almost the same carbon formation as the Ae-LDH tested over 6 h of reaction.

4. Conclusions

According to the powder XRD patterns, it can be concluded that a hydrotalcite structure was formed and the thermal treatment did not destroy completely the structure of the precursor.

The TPR and powder XRD patterns indicated that all catalysts are formed basically by a mixture of hydrotalcite, Co_3O_4 , Co_2MgO_4 and CoAl_2O_4 phases.

It has been demonstrated that cobalt catalysts obtained from hydrotalcite exhibit good activity and stability for methane steam reforming. The low quantity of carbon formed on the Ae-catalyst surface suggests that the anion-exchange method provides a more homogeneous distribution of the active phase than that obtained by the other methods.

Acknowledgements

The authors are grateful to the Brazilian federal research funding council, CNPq, for financial support and to the Department of Chemical Engineering at the Federal University of São Carlos.

References

- [1] O. Yamazaki, K. Tomishige, K. Fujimoto, *Appl. Catal. A: Gen.* 136 (1996) 49–56.
- [2] M.V. Twigg, *Catalyst Handbook*, second ed., Manson Publishing, England, 1996.
- [3] M.P. Makoa, N.J. Coville, V.D. Sokolovskii, *Catal. Today* 49 (1999) 11–16.
- [4] T. Shishido, M. Sukenobu, H. Morioka, R. Furukawa, H. Shirahase, K. Takehira, *Catal. Lett.* 73 (2001) 21–26.
- [5] E. Ruckenstein, H.Y. Wang, *J. Catal.* 205 (2002) 289–293.
- [6] S. Casenave, H. Martinez, C. Guimon, A. Aurox, V. Hulea, A. Cordoneanu, E. Dumitriu, *Thermochim. Acta* 379 (2001) 85–93.
- [7] K. Bahranowski, G. Bueno, V.C. Corberán, F. Kooli, E.M. Serwicka, R.X. Valenzuela, K. Wcisło, *Appl. Catal. A: Gen.* 185 (1999) 65–73.
- [8] A. Vaccari, *Catal. Today* 41 (1998) 53–71.
- [9] A.I. Tsyganok, K. Suzuki, S. Hamakawa, K. Takehira, T. Hayakawa, *Catal. Lett.* 77 (2001) 75–86.
- [10] A.I. Tsyganok, T. Tsunoda, S. Hamakawa, K. Suzuki, K. Takehira, T. Hayakawa, *J. Catal.* 213 (2003) 191–203.
- [11] A. Fonseca, E.M. Assaf, *J. Power Sources* 142 (2005) 154–159.
- [12] E. Ruckenstein, H.Y. Wang, *Catal. Lett.* 73 (2001) 99–105.
- [13] L. Chmielarz, P. Kuśtrowski, A. Rafalska-Łasocha, R. Dziembaj, *Thermochim. Acta* 395 (2003) 225–236.
- [14] JCPDS—Joint Committee on Powder Diffraction Standards, International Center of Diffraction Data, Pensilvânia USA, 1994 (CD-ROM).
- [15] A.A. Khassin, T.M. Yurieva, G.N. Kustova, I.S. Itenberg, M.P. Demeshkina, T.A. Krieger, L.M. Plyasova, G.K. Chermashentseva, V.N. Parmon, *J. Molec. Catal. A: Chem.* 168 (2001) 193–207.
- [16] H.Y. Wang, E. Ruckenstein, *Appl. Catal. A: Gen.* 209 (2001) 207–215.